PHYSICAL REVIEW D **92,** 094022 (2015)

Interacting ensemble of the instanton-dyons and the deconfinement phase transition in the SU(2) gauge theory

Rasmus Larsen and Edward Shuryak

Department of Physics and Astronomy, Stony Brook University, Stony Brook, New York 11794-3800, USA

(Received 4 September 2015; published 19 November 2015)

Instanton-dyons, also known as instanton-monopoles or instanton-quarks, are topological constituents of the instantons at nonzero temperature and holonomy. We perform numerical simulations of the ensemble of interacting dyons for the SU(2) pure gauge theory, using standard Metropolis Monte Carlo and integration over parameter methods. We calculate the free energy as a function of the holonomy (logarithm of the Polyakov line), the dyon densities, and the Debye mass, and find its minima as a function of those parameters. We show that the backreaction on the holonomy potential does generate confinement, provided the density is sufficiently high (or the temperature sufficiently low). We then report various properties of the self-consistent ensembles as a function of temperature.

DOI: 10.1103/PhysRevD.92.094022 PACS numbers: 12.38.Aw

I. INTRODUCTION

QCD description of strongly interacting matter at finite temperature T has originated from the 1970s. At first, its high temperature phase—known as quark-gluon plasma, QGP—has been studied using weak coupling methods, see e.g. reviews [1,2]. The interest then switched to nonperturbative phenomena, related with the topological solitons of various dimensionality and two basic nonperturbative phenomena: confinement and chiral symmetry breaking. Instantons [3], the Euclidean 4-dimensional topological solitons, have at high T the sizes $\rho \sim 1/T$ and appear with the probability

$$\frac{n_{\text{instantons}}}{T^4} \sim \exp[-8\pi^2/g^2(T)] \sim \left(\frac{\Lambda}{T}\right)^b, \qquad (1)$$

where the power is the one loop beta function coefficient, $b = 11N_c/3$ for $SU(N_c)$ gauge theory. So, at high T the density is small and the topological solitons are unimportant. Conversely, as T decreases, the instanton density rapidly grows, till they become an important ingredient of the gauge fields in the QCD vacuum. Index theorems ensure existence of the fermionic zero modes of topological solitons. Those generate the so-called 't Hooft effective interaction of $2N_f$ fermions, which explicitly violates the $U_A(1)$ chiral symmetry. Furthermore, collectivization of the zero modes create the so-called zero mode zone of quasizero eigenstates, which break spontaneously the $SU(N_f)$ chiral symmetry. Although those states include only a tiny subset of all fermionic states in lattice numerical simulations, they are the key elements of the chiral symmetry breaking and the hadronic spectroscopy. The so-called interacting instanton liquid model (IILM) has been developed, including 't Hooft interaction to all orders, for a review see [4].

The presence of the topological solitons in the vacuum has been related with the issue of confinement. In particular, in [5,6] it has been noted that superposition of *regular gauge* instantons, or merons, can disorder the Wilson loop to an area law. These effects are due to accumulated contributions of distant solitons, which are assumed to have long-range (1/r) tails of the gauge fields. However, already using more appropriate configurations of *singular gauge* instantons, with fields decaying as $1/r^3$, one finds only finite and nonconfining heavy-quark potential [7]. Similar confining effect can be generated by the instanton-dyons [8]: in this case most components of the gauge field obtain a mass due to nonzero holonomy, but the diagonal (Abelian) gluons do not and remain massless. So again, there are $1/r$ tails of the solitons, also disordering the Wilson loop.

Some IR effects can be argued to be artifacts since all physical correlators in the vacuum are exponentially decaying with distance. In particular, the holonomy vacuum expectation value (VEV) has a certain effective potential, and its second derivative at the minimum provides a nonzero Debye screening mass M_D. If included consistently, it leads to exponentially decaying tails and eliminates infrared artifacts. However, Wilson lines can also be disordered by magnetic (center) vortices [9] not related to the IR effects: in this paper we will not discuss this aspect of confinement.

In this paper we focus instead on derivation of the (local and average) effective holonomy potential. By "confinement" we will below imply its modification with temperature, such that at $T < T_c$ the minimum corresponds to the "confining" value of the holonomy. More specifically, the holonomy potential contains two terms. One is the well known Gross-Pisarski-Yaffe one-loop effective potential, coming from QGP effects on holonomy. The second term —the main object discussed below—is due to backreaction of the instanton-dyons. As we show below, *together*

they produce a holonomy potential with minimum shifting with the dyon density, eventually to its confining value. The second derivative—the Debye mass—is in general nonzero. This means there is always exponential screening, and thus the long-range problem discussed in the papers mentioned is in principle solved. For the same reason long-distance effects are relatively small in the simulations.

As the temperature decreases from the high-T regime, another important phenomenon is the appearance of nontrivial expectation value of the Polyakov line. For the simplest SU(2) gauge theory we will be discussing in this work, it is related to the so-called holonomy parameter by $\langle P\rangle = \cos(\pi\nu)$ (for explicit notations see Appendix A). While at high T it vanishes $\nu \to 0$ and the Polyakov line vacuum expectation value is $\langle P\rangle = 1$, at temperatures at and below the critical value T_c it reaches the so called "confining value" $\nu = 1/2$ at which the Polyakov line vanishes itself. This leads to switching out quark and gluon degrees of freedom, and transition from QGP to hadronic matter. Study of the instantons at nonzero holonomy has lead Lee,Lu,van Baal and Kraan [10,11] to the so-called KvBLL caloron solution, which revealed that at $\nu \neq 0$ the instantons get split into N_c (number of colors) (anti)dyons, (anti)self-dual 3d solitons with nonzero (Euclidean) electric and magnetic charges. (Details are in Appendix B.) Because of the long-range nature of forces between these objects, we will thus refer to the instanton-dyon ensemble as the "dyonic plasma."

Unlike instantons, protected by topology, the instanton-dyons interact directly with the holonomy. Diakonov [12] suggested that backreaction of the dyon free energy on holonomy is responsible for confinement phase transition but was unable to show it.

Poppitz, Schaefer and Unsal [13] had shown that instanon-dyon confinement does occur in a very specific "controlled setting," a supersymmetric theory compactified on $R^3 \otimes S^1$ with a small spatial circle and periodic fermions. The smallness of the circle, like high T, makes the coupling weak. The periodic fermions preserve supersymmetry and cancel the Gross-Pisarski-Yaffe (GPY) holonomy potential $V_{\rm GPY}(\nu)$, which allows confinement to be induced even by an exponentially small density of the dyons. These authors have been able to trace the crucial effect to the repulsive dyon-antidyon interaction inside the dyon-antidyon pairs (which they call "bions").

Simple phenomenological model showing that repulsive interaction between them, modeled by an excluded volume, has been proposed for QCD-like theories by Shuryak and Sulejmanpasic [14], which reached qualitative description of the deconfinement phase transition and other properties of the thermal $SU(2)$ pure gauge system above T_c, in qualitative agreement with available lattice data. We will discuss a similar model in Sec. II, before we embark on numerical simulations.

Although the interaction between the instanton-dyons has been studied for a long time, the leading-order effect—classical dyon-antidyon interaction has been missing. The corresponding studies, deriving the so-called "streamline" set of configurations via the gradient flow method, has been done in our previous work [15]. While it turns out to be weak in relative terms $\delta S \ll S$ but, it is still parametrically enhanced $\delta S \sim 1/g^2$ because of being classical. What matters for the present work is that interaction $\delta S = O(1)$ is large enough to induce significant correlations in the ensemble.

Liu, Shuryak and Zahed [16] have recently shown that one can incorporate this classical interaction by the mean field techniques, provided the ensemble is dense enough to generate sufficient screening. In terms of the temperature, their treatment applies only for some interval of temperatures $T < T_c$.

The goal of our present work is to study the instanton-dyon ensemble by the direct Monte-Carlo simulation, without the *mean field* or any other approximations. As we will show, this will allow us to cover any density regimes, from dilute to dense, and follow the transformation of the holonomy potential in details. We thus can discuss both sides of the deconfinement phase transition. To complement [16], we will mainly focus on temperatures $T \geq T_c$.

Technically, the details of the setting to a large extent follow the first Monte-Carlo simulations of the instanton-dyon plasma by Faccioli and Shuryak [17]. One major difference is the inclusion of the classical "streamline" interaction which were not known at the time of that work. The other is that paper focused on the role of fermions and chiral symmetry breaking rather than confinement. (We expect to report on our next paper, with fermions, soon.)

The paper is structured as follows: standard information about our notations, the holonomy potential and the instanton-dyons are delegated to sections of the Appendix. We start in Sec. II by introducing a simple model which illustrates the main physics under discussion. Then in Sec. III we explain the setting of the simulations, the interaction between the instanton-dyons and the moduli spaces which provides the measure in the partition function. In Sec. IV we describe how we make the actual simulations and evaluate the free energy. The backreaction of the ensemble on the holonomy potential is described in Sec. V, which is followed by "self-consistency" study of the parameters in the Sec. VI. The physical results are summarized in the Sec. VII: those include the holonomy potential and the screening masses, as well as the densities of all types of dyons.

II. AN EXCLUDED VOLUME MODEL

To understand the main physics involved and the qualitative behavior of the ensemble, including the confinement phase transition, we start by a discussion of a

simplified model in which the only interaction is the repulsive core, making the volume occupied by each particle unavailable to others. It is similar in spirit to that proposed by Shuryak and Sulejmanpasic [14], but is somewhat closer technically to the simulations to follow.

We work with dimensionless quantities, defining the 3-volume as $\tilde{V}_3 = T^3 V_3$, the density $n_i = \frac{N_i}{\tilde{V}_3}$, and the free energy density as $\frac{F}{T\tilde{V}_3} = f$. More information on units and notations can be found in Appendix.

The effect of the excluded volume is accounted for in a very schematic way, by cutting off the partition function when the amount of available volume vanishes. The volume of the M and L dyons scale by $1/\nu^3$ and $1/\bar{\nu}^3$, respectively, with $\bar{\nu} = 1 - \nu$. We thus define the partition function as a sum limited from above by some "close packing" condition

$$Z = \sum_{M,L}^{\tilde{V}_3/(\tilde{V}_0)<M/\nu^3+L/\bar{\nu}^3} \exp\left(-\tilde{V}_3 \frac{4\pi^2}{3}\nu^2\bar{\nu}^2\right) \times \left[\frac{1}{M!L!}(\tilde{V}_3 d_\nu)^M (\tilde{V}_3 d_{\bar{\nu}})^L\right]^2 \quad (2)$$

$$d_\nu = \Lambda \nu^{8\nu/3} S^2 \exp(-S\nu) \quad (3)$$

$$S = \frac{8\pi^2}{g^2}. \quad (4)$$

Without the upper limit, the free energy density is simply $\log(Z)/\tilde{V}_3 \to -\frac{4\pi^2}{3}\nu^2\bar{\nu}^2 + 2(d_\nu + d_{\bar{\nu}})$, the perturbative Gross-Pisarski-Yaffe (GPY) potential plus the contribution of the noninteracting dyons. In this noninteracting limit, the parameter d_ν—the semiclassical dyon amplitude—coincides with their density. The parameter S is in fact the classical action of the caloron, or $L + M$ system. The square comes from assuming the same amount of dyons and antidyons.

In the confining phase, $\nu = \bar{\nu} = 1/2$, all dyons have the same sizes, and it is easy to introduce the excluded volume, for N dyons via

$$\tilde{V}_3^N \to \tilde{V}_3(\tilde{V}_3 - V_{\text{excluded}})\ldots(\tilde{V}_3 - (N-1)V_{\text{excluded}}).$$

However, in general L, M dyons have different sizes, the analogous expression becomes cumbersome. Experimenting with those, we observe that similar results are obtained by simply cutting out the sum at "closed packing," when there is no volume left, $\tilde{V}_3 < \tilde{V}_0(M/\nu^3 + L/\bar{\nu}^3)$, where $\tilde{V}_0$ is the excluded volume normalized for a dyon at $\nu = 1$.

Using Sterlings formula $n! \approx \sqrt{2\pi n}(\frac{n}{e})^n$ for a large volume, we rewrite the sum as

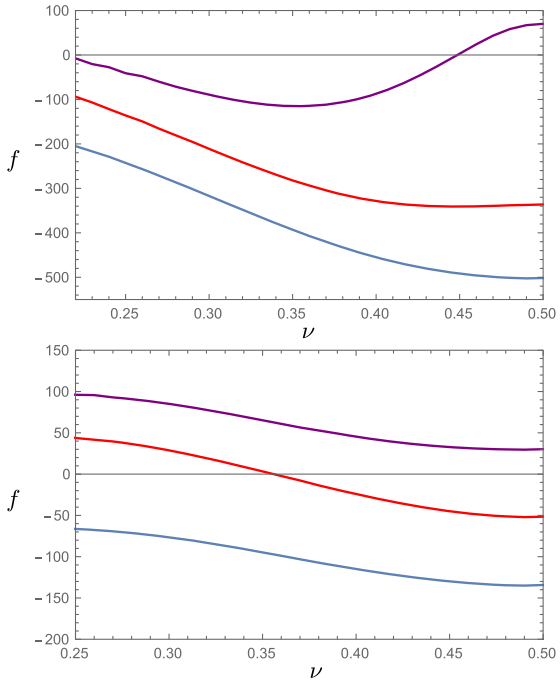

FIG. 1 (color online). Free energy density f as function of holonomy ν, for $\Lambda = 0.5$ and $\tilde{V}_0 = 0.3$, for upper and $\tilde{V}_0 = 0.6$ for the lower plot. Three curves correspond to $g = 4$, 3.5, 3, bottom to top, in the upper figure and $g = 4$, 3.5, 3.25 in the bottom one. It is seen how the maximum as a function of g goes further and further toward the confining value of $1/2$ as g goes up, and S and T go down.

$$Z = \sum_{M,L}^{\tilde{V}_3/(\tilde{V}_0)<M/\nu^3+L/\bar{\nu}^3} \exp\left[-\tilde{V}_3\left(\frac{4\pi^2}{3}\nu^2\bar{\nu}^2 - 2n_M \ln\left[\frac{d_\nu e}{n_M}\right] - 2n_L \ln\left[\frac{d_{\bar{\nu}} e}{n_L}\right]\right)\right]. \quad (5)$$

The free energy given by $F(\nu) = -T\log Z$ depends on ν, located in the cutoff, in the dyon parameter d_ν, and in the GPY potential V_{GPY}. If dominant, the GPY term would select trivial holonomy $\nu = 0$ or $\bar{\nu} = 0$, so to push for a nontrivial $\nu \sim 1/2$ needed for confinement, the dyon densities should be large enough.

The expression (5) is put into *Mathematica* and the maximum is found, for large enough volume, say $V = 900$. One finds a sharp peak in N distribution, defining the density. Finding the maximum as we vary ν, we get $f(\nu) = -\log Z/\tilde{V}_3$ plotted in Fig. 1. At smaller g (larger S and higher T) the dyons are more suppressed and the free energy density f has a minimum at smaller ν. For increasing coupling g (decreasing S and T), the minimum shifts from zero, eventually to its confining value $\nu = 1/2$. For twice larger excluded volume the density may get too small to have confinement with physically meaningful—negative—f.

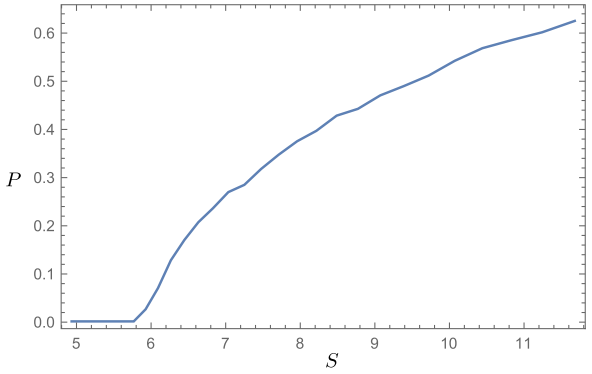

FIG. 2 (color online). Polyakov loop P as a function of action parameter S for $\Lambda = 0.5$ and $\tilde{V}_0 = 0.3$.

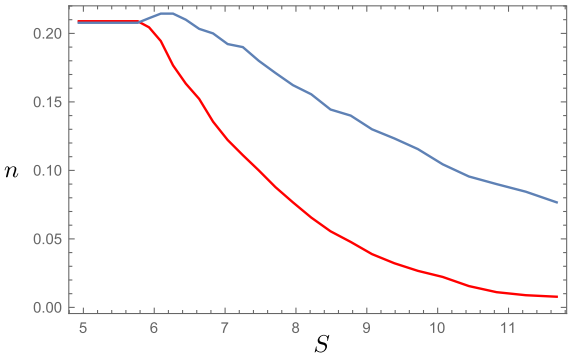

FIG. 3 (color online). Densities n_i of $i = M$ or $i = L$ dyons as a function of the action parameter S, for $\Lambda = 0.5$ and $\tilde{V}_0 = 0.3$. Note that the two densities are different at $S > 6$.

A more familiar plot is obtained if, instead of plotting ν one plots the average Polyakov loop $\langle P \rangle = \cos(\pi\nu)$, versus S, see Fig. 2. The parameter S grows monotonously with T and thus can be mapped to it (see details in Appendix A). So, in this model the Polyakov loop continuously goes to 0—the confinement regime—at some critical S_c, slightly smaller than 6.

In Fig. 3 we show the densities of different type (M and L) dyons, different at above the deconfinement transition. Direct evidences for $n_M > n_L$ in the deconfined phase have been found on the lattice. We will see similar plots from the numerical simulations below: those of course would include the dyon interactions.

III. THE INSTANTON-DYON INTERACTIONS

The *leading order* classical dyon-antidyon interaction, recently studied in our previous paper [15] are the central new elements of this paper. We use a slightly different parametrization of it

$$\Delta S_{D\bar{D}} = -2\frac{8\pi^2\nu}{g^2}\left(\frac{1}{x} - 1.632e^{-0.704x}\right)$$
$$x = 2\pi\nu r T, \tag{6}$$

for distances larger than $x > 4$, the repulsive core size. At distance $x = 4$ the streamline terminates a metastable configuration, followed by annihilation of the magnetic charges.

If dyons are put at smaller distances, they repel till distance 4, before annihilation. Those configurations were not yet studied in detail, and thus our potential for $x < 4$ constitutes a reasonable guess. Below distance $x_0 = r_0 T(2\pi\nu)$ the potential is described by

$$\Delta S_{D\bar{D}} = \frac{\nu V_0}{1 + \exp\left[\sigma(x - x_0)\right]}, \tag{7}$$

referred to as a "core." Its scale by ν is due to general scaling behavior of the dyon sizes.

Let us also recall the long-distance behavior of the potentials. Self-dual soliton interacting with anti-self-dual one has Abelian electric and magnetic forces canceling each other. Another long-range interaction comes via A_4 and the nonlinearity of the field strength tensor. Its coefficient is fixed in another channel, $L + M$ (calorons) where both electric and magnetic Abelian effects are attractive, and yet the total interaction is zero due to PBS protection

$$V_{LM} = (e_1 e_2 + m_1 m_2 - 2h_1 h_2)\frac{4\pi}{g^2}\frac{1}{r} = 0. \tag{8}$$

Returning to $M\bar{L}, L\bar{M}$ channel, one expects the non-Abelian term simply to change sign. This conclusion that has been checked by us numerically, see latest version of [15].

The volume element of the metric in the space of collective variables is used in the form of the so-called Diakonov determinant

$$\sqrt{g} = \det G \tag{9}$$

$$G = \delta_{mn}\delta_{ij}\left(4\pi\nu_m - 2\sum_{k\neq i}\frac{1}{T|x_{i,m} - x_{k,m}|} + 2\sum_{k}\frac{1}{T|x_{i,m} - x_{k,p\neq m}|}\right) + 2\delta_{mn}\frac{1}{T|x_{i,m} - x_{j,n}|} - 2\delta_{m\neq n}\frac{1}{T|x_{i,m} - x_{j,n}|}, \tag{10}$$

where $x_{i,m}$ denote the position of the ith dyon of type m. This form is an interpolation of the exact metric between a M and L dyon, true at any distance, with the metric of the two dyons of same type at large distances. We introduce a cutoff on the separation via $r \to \sqrt{r^2 + \text{cutoff}^2}$, such that for one pair of dyons of same type, the diagonal goes to 0 for $\nu = 0.5$, instead of minus infinity. We use the same metric for the antidyons also.

When the density of M and L dyons are different, the total electric charge is nonzero. We therefore regularize all the Coulombic terms by certain screening $r \to re^{M_D rT}$,

referred to as the Debye mass. With this the interaction is given by

$$\Delta S_{D\bar{D}} = \frac{8\pi^2\nu}{g^2}\left((e_1e_2 - 2h_1h_2)\frac{1}{x} + m_1m_2\frac{1}{x}\right)e^{-M_D rT}$$
$$x = 2\pi\nu rT, \tag{11}$$

for r larger than the core of size $x_0/(2\pi\nu T)$ for all combinations except between dyons and their antidyon. For the dyon antidyon potential we have

$$\Delta S_{D\bar{D}} = -2\frac{8\pi^2\nu}{g^2}\left(\frac{1}{x} - 1.632e^{-0.704x}\right)e^{-M_D rT}$$
$$x = 2\pi\nu rT. \tag{12}$$

We include the core for both dyon antidyon interactions, but also for dyon dyon interactions as it is necessary for stability of the simulations. We hope that such an interaction can be found due to corrections to the metric between dyons of the same type.

$$\Delta S_{D\bar{D}} = \frac{\nu V_0}{1 + \exp\left[\sigma T(x - x_0)\right]}$$
$$x = 2\pi\nu rT. \tag{13}$$

IV. THE SETUP

Like in [17], instead of the usual toroidal box with periodic boundary conditions in all coordinates, our simulations have been done on a S^3 sphere (in four dimensions), to simplify treatment of the long range Coulombic forces. In this pilot study we fix the total number of dyons to 64. We do not use supercomputers or clusters, relying instead on multiple cores of standard GPU's of one standard computer.

The radius of the sphere together with the ratio of M dyons to L dyons have been used to change their density.

Iteration of the system is defined as a loop in which each dyon has had its position changed and the new action has then been accepted with the probability of $\exp(-\Delta S)$ via the Metropolis algorithm. The typical number of iterations, for equilibration is 400 and productive runs after equilibration are typically 1600 iterations.

In order to get the free energy we also use a standard method. One can differentiate with respect to an auxiliary parameter λ introduced in front of the action and get

$$e^{-F(\lambda)/T} = \int Dx \exp(-\lambda S(x)) \tag{14}$$

$$\frac{\partial F}{\partial \lambda} = T\langle S\rangle. \tag{15}$$

Since the free energy at $\lambda = 0$ is known analytically, one can integrate up to get the free energy at $\lambda = 1$. When we do this we of course need to be careful about regions with a quick change in the action.

For the calculation of $\det G$ it has been observed by Bruckmann *et al.* [18] that it only make sense if all eigenvalues are positive. It was observed [18] that, for randomly placed dyons this is typically not the case, unless density is very low. In [16] this issue has been discussed further, with a conclusion that the Diakonov determinant can remain positive definite at higher densities needed, but only provided certain correlations in the dyon locations are enforced. We have therefore used the householder QR algorithm together with tri-diagolization of the matrix G [19] to find the eigenvalues. We also redefine the potential as follows:

If all eigenvalues are positive

$$V_D = -\log[\mathrm{Det}(G)]\colon\ V_D < V_{\max} \tag{16}$$

$$V_D = V_{\max}\colon\ V_D > V_{\max} \tag{17}$$

and for one or more negative eigenvalues

$$V_D = V_{\max}. \tag{18}$$

The excluded volume from the regions of negative eigenvalues are there, yet at the same time we do not create a region where the configuration can be trapped inside the region of negative eigenvalues. Excluded volume induces strong variation of the free energy at small λ: so we found it necessary to integrate the free energy up to $\lambda = 0.1$ finely with 10 points. From $\lambda = 0.1$ to $\lambda = 1$ we use 9 points. $V_{\max} = 100$ was used.

In the simulation, all interactions are assumed to have Yukawa-like large distance behavior with certain Debye screening mass M_D. Since our "box size" can be defined as the distance between poles of our sphere, $\pi * r$. In the smallest box we have a box size of about 4 units. The smallest Debye mass employed is, in the same units, 2. Thus the exponential tails are $e^{-M_D r} = e^{-8}$, and all IR artifacts are well suppressed.

That finite volume effects are not important was tested on a few configurations as shown in Fig. 4, since it is not possible to do it for all configurations due to the computational power needed. We find that the configurations do indeed give the same results for double the volume in the area of interest, and only at densities higher than explored in this paper do we see a difference. The difference at higher densities is due to the sharpened behavior of $\langle S(\lambda)\rangle$, and should be fixed in case one wants to do higher total number of dyons, by increasing the density of points in the integration to obtain the free energy F.

V. THE DYON BACK REACTION: HOLONOMY POTENTIAL

Lattice gauge simulations had shown how the peak of the holonomy distribution shifts to its confining value at $T < T_c$. The corresponding effective potential $V(\nu, T)$

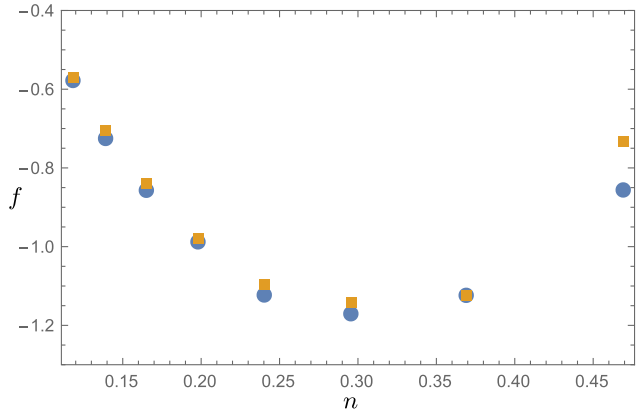

FIG. 4 (color online). Free energy density f as a function of density n for $N_{\rm Total}=64$ (filled blue circle) and $N_{\rm Total}=128$ (yellow square) at $\nu=0.5$, $M_D=2$, $S=6$ and $n=n_M=n_L$. Volume effects are seen to not be important in the region of interest around $n=0.3$ and difference is expected to come from the sharper shape of $\langle S(\lambda)\rangle$ in the case of $N_{\rm Total}=128$, which require a higher amount of points to obtain the free energy F.

has been numerically studies and parametrized, used in various models such as the so called Polyakov-Nambu-Jona-Lasinio model (PNJL).

Now our task is to derive this potential, stemming from the backreaction of the instanton-dyons. We add the perturbative GPY potential $V_{\rm GPY}$ eq. (A2) to the dyon free energy obtained from our simulations and determine the total free energy of the system (obviously, assuming that there are no other relevant nonperturbative contributions). The dyon-induced partition function is further split into two factors: one containing all factors which depend on parameters unchanged in the simulations, and the second one related to dyons's collective variables.

$$Z = Z_{\rm unchanged} Z_{\rm changed}. \tag{19}$$

The weight for one caloron ($L+M$ pair) was explicitly calculated in [20]: at zero holonomy it agrees with the instanton result by 't Hooft. Part of the answer is the factor coming from the metric volume element $\sqrt{g}$ in the space of L, M collective variables. Later Diakonov [12] combined this result with the previously known answer for the metric of two monopoles of the same kind (e.g. M, M pair) into an elegant expression for any number of L, M dyons now called Diakonov determinant $\det G$.

Taking the dilute limit $r_{12}\to\infty$ in both cases both formulas reduce to the same r_{12} dependence and one finds that the caloron weight from [20] needs to be divided by the factor $(4\pi\nu)(4\pi\bar\nu)$ (see Appendix C)

$$Z_{\rm unchanged} = \frac{\Lambda^2}{(4\pi)^2}\left(\frac{8\pi^2}{g^2}\right)^4 e^{-\frac{8\pi^2}{g^2}}\nu^{\frac{8\nu}{3}-1}\bar\nu^{\frac{8\bar\nu}{3}-1} \times \exp\left(-\tilde V_3\frac{4\pi^2}{3}\nu^2\bar\nu^2\right). \tag{20}$$

Note that at the trivial holonomy $\nu\to 0$ limit, $Z_{\rm unchanged}$ is $\sim 1/\nu$: it is to be canceled by the diagonal part of the $\det(G)$ in the second part.

We need to do the simulation for different amounts of M and L dyons. We divide the weight into a M part and a L part, and sum over all number of particles

$$Z_{\rm unchanged} = \sum_{N_M,N_L}\exp\left(-\tilde V_3\frac{4\pi^2}{3}\nu^2\bar\nu^2\right) \times\left[\frac{1}{N_M!}\left(\Lambda\tilde V_3\left(\frac{8\pi^2}{g^2}\right)^2 e^{-\frac{\nu 8\pi^2}{g^2}}\nu^{\frac{8\nu}{3}-1}/(4\pi)\right)^{N_M}\right]^2 \times\left[\frac{1}{N_L!}\left(\Lambda\tilde V_3\left(\frac{8\pi^2}{g^2}\right)^2 e^{-\frac{\bar\nu 8\pi^2}{g^2}}\bar\nu^{\frac{8\bar\nu}{3}-1}/(4\pi)\right)^{N_L}\right]^2, \tag{21}$$

where we use that the amount of dyons and antidyons is the same. We simplify this as

$$Z_{\rm unchanged} = \sum_{N_M,N_L}\exp\left(-\tilde V_3\frac{4\pi^2}{3}\nu^2\bar\nu^2\right) \times\left[\frac{1}{N_M!}(\tilde V_3 d_\nu)^{N_M}\right]^2\left[\frac{1}{N_L!}(\tilde V_3 d_{\bar\nu})^{N_L}\right]^2$$
$$d_\nu = \Lambda\left(\frac{8\pi^2}{g^2}\right)^2 e^{-\frac{\nu 8\pi^2}{g^2}}\nu^{\frac{8\nu}{3}-1}/(4\pi). \tag{22}$$

$Z_{\rm changed}$ is the interactions explained in Sec. III and thus also depends on the number of particles

$$Z_{\rm changed} = \frac{1}{\tilde V_3^{2(N_L+N_M)}}\int D^3x\,\det(G)\exp(-\Delta D_{D\bar D}(x))$$
$$\Delta f \equiv -\log(Z_{\rm changed})/\tilde V_3, \tag{23}$$

normalized such that $Z_{\rm changed}=1$ for no interactions included. Combining $Z_{\rm changed}$ with $Z_{\rm unchanged}$ we get in the limit $\tilde V_3\to\infty$

$$Z = \sum_{N_M,N_L}\exp\left(-\tilde V_3\left[\frac{4\pi^2}{3}\nu^2\bar\nu^2 - 2n_M\ln\left[\frac{d_\nu e}{n_M}\right] - 2n_L\ln\left[\frac{d_{\bar\nu}e}{n_L}\right]+\Delta f\right]\right). \tag{24}$$

For $\tilde V_3\to\infty$ the partition function is completely dominated by the maximum of the exponent. Finding the free energy corresponds to finding the minimum of

$$f = \frac{4\pi^2}{3}\nu^2\bar\nu^2 - 2n_M\ln\left[\frac{d_\nu e}{n_M}\right] - 2n_L\ln\left[\frac{d_{\bar\nu}e}{n_L}\right]+\Delta f. \tag{25}$$

Note that as the dyon density increases, the potential changes its shape, as shown in Fig. 5, producing a

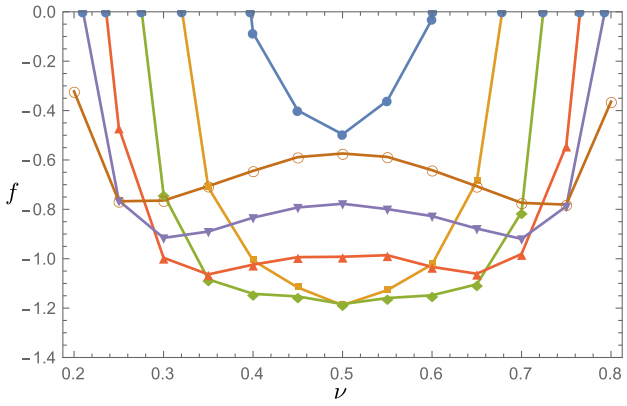

FIG. 5 (color online). Free energy density f as a function of ν at $S = 6$, $M_D = 2$ and $N_M = N_L = 16$. The different curves corresponds to different densities. Filled circle $n = 0.53$, square $n = 0.37$, diagonal $n = 0.27$, upward triangle $n = 0.20$, downward triangle $n = 0.15$, open circle $n = 0.12$. Not all densities are shown.

nontrivial minimum at $\nu \neq 0$. Furthermore, at high density this minimum moves to $\nu = 1/2$, the confining value.

VI. SELF-CONSISTENCY

The partition function we simulate depends on several parameters, changed from one simulation set to another. Those include (i) the number of the dyons N_M, N_L; (ii) the radius of the S^3 sphere r; (iii) the action parameter S; (iv) the value of the holonomy ν, (v) the value of the Debye mass M_D; (vi) the auxiliary factor λ, which is then integrated over as explained in Sec. IV.

In principle, the aim of our study is to obtain the dependence of the free energy on all of those parameters (i–v). While the practical cost of the simulations restricts the number of points one can study, we still had generated more than hundred thousand runs and multiple plots. However, most of it neither can nor should be included in the paper. Since our physics goal is to understand the backreaction of the dyon ensemble on the holonomy, we study the range of holonomies, from $\nu = 0$ to $\nu = 1/2$, and only then locate its minimum. As for the Debye mass, we will find it from the potential minimum and then show only the "self-consistent" input set.

What we actually need to describe at the end is not the free energy in the whole multidimensional space of all parameters, but the location of the free energy minima. The resulting set should be of codimension 1, since the original physical setting of the problem—the gauge theory at finite temperature—has only one input parameter, T.

Using the definition of the Debye mass $\frac{g^2}{2V}\frac{\partial^2 F}{\partial^2 v} = M_D^2$ for fixed density we get the configurations response to changing the holonomy which is the Debye mass. We require that the used value for the Debye mass is the same as the one found from the derivative of F, or at least not more than 0.4 below the used value.

The results shows that as the Debye mass goes toward zero around the phase transition the only configuration that is consistent with this is that of equal M and L dyons.

VII. THE PHYSICAL RESULTS

We now show only the results which fulfill the self-consistency requirement. Without fermions the results are symmetric in $\nu \to 1 - \nu$ and are therefore shown only for $\nu \leq 1/2$. We have included the Diakonov determinant, though its impact is not too great due to the not so small Debye mass which has been calculated using 3 points. The results here are shown for a wall of $x_0 = 2$, which was chosen in order to have a large enough density of dyons to overcome the perturbative potential, without completely making the GPY potential irrelevant. We used $\Lambda = 1.5$ to obtain a phase shift around $S = 6$. Action is related to temperature as explained in Appendix A. This should of course be fitted to numerical data, but the present data on dyons does not have a high enough efficiency of detection to do this. The action goes up to $S = 13$, beyond this value the number of L dyons becomes too close to 1, and we would need a higher total number of dyons to proceed.

Due to the repulsive Coulomb term between dyons and antidyons of different type, the free energy preferred to have a large Debye mass due to cutting off this repulsion. This meant that when the free energy spectrum as a function of holonomy for a fixed density becomes flat, the small Debye mass created a rise in energy. This resulted in a small jump in holonomy, since the configurations with holonomy $\nu = 0.5$ but with slightly higher density than the flat ones, would end up with a smaller free energy. As a result we do not get a completely smooth transition, though that is hidden by the size of the errors as seen in Fig. 6. It also means that at $S = 6$ the Debye mass never goes completely to zero, as shown in Fig. 7, and the density goes slightly more up also as shown in Fig. 8. In Fig. 9 we show S-dependence of the free energy itself.

When we are in the confined region we observe the free energy for a fixed density as a single minimum in the middle at $\nu = 0.5$. As the action S increases, the density of dyons decrease and it becomes more favorable to have some bigger, but lighter dyons, thus shifting the minimum away from the confining value of the Polyakov loop, $P = 0$, as can be seen in Fig. 10 for $S = 6$, 7, 9. This, at the same time, makes the lighter M dyons more abundant than the more heavy L dyons.

Due to the size of the Debye mass, the correlation functions behaves as that in a liquid, with a cutoff at small range. We show the case for $S = 6$ in Fig. 11 for MM and ML. Note the correlation function C_{MM} vanishes at small distances due to the core. The other correlation function C_{ML} for ML, displays attraction even at small distances, tripling the density at $r = 0$. The integrated number of particles in the region in which the correlation function

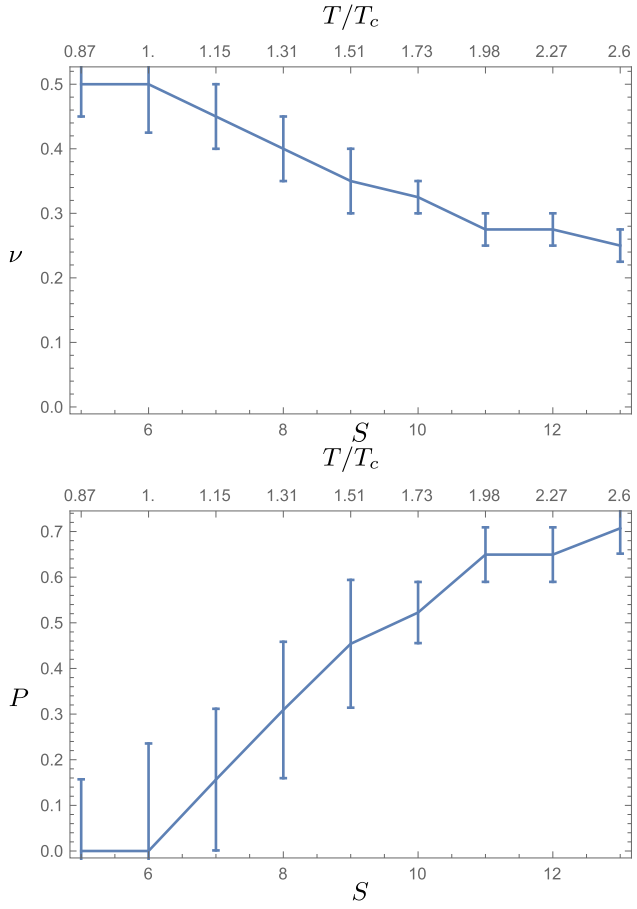

FIG. 6 (color online). Self-consistent value of the holonomy ν (upper plot) and Polyakov line (lower plot) as a function of action S (lower scales), which is related to T/T_c (upper scales). The error bars are estimates based on the fluctuations of the numerical data.

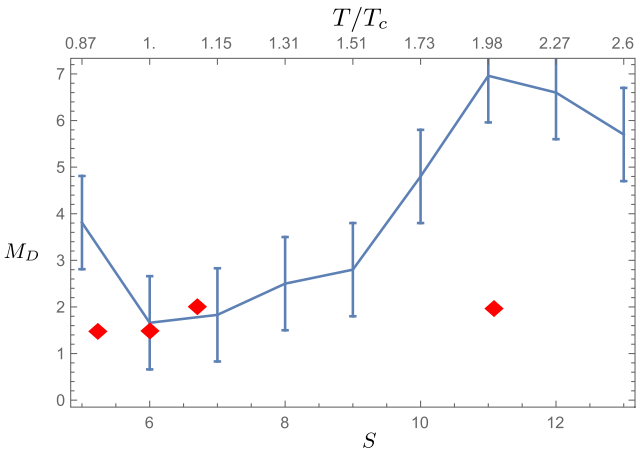

FIG. 7 (color online). Self-consistent value of the Debye Mass M_D as a function of action S (lower scale) which is related to T/T_c (upper scale). The error bars are estimates based on the fluctuations of the numerical data. Points represent lattice data from [21] as a function of T/T_c.

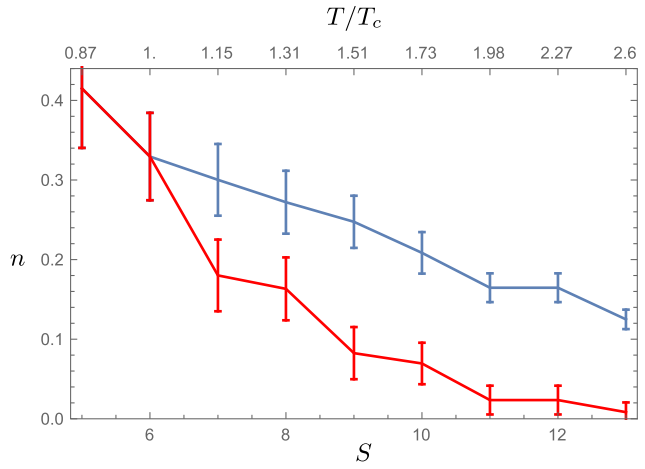

FIG. 8 (color online). Density n (of an individual kind of dyons) as a function of action S (lower scale) which is related to T/T_c (upper scale) for M dyons(higher line) and L dyons (lower line). The error bars are estimates based on the density of points and the fluctuations of the numerical data.

$C_{ML}(r) > 1$ is 0.50 particles, while for C_{MM} it corresponds to 0.34 particles: thus the difference is not that large.

VIII. POSSIBLE IMPROVEMENTS

In this round of simulations we have been able to describe how the deconfinement phase transition happens. We were reaching for a self-consistent description of the system, in which all parameters being at the values corresponding to the free energy minima.

Yet the self-consistency of the calculation remains in a way incomplete. In this section we make one more step toward it, but, as we will soon see, further ones may perhaps be needed.

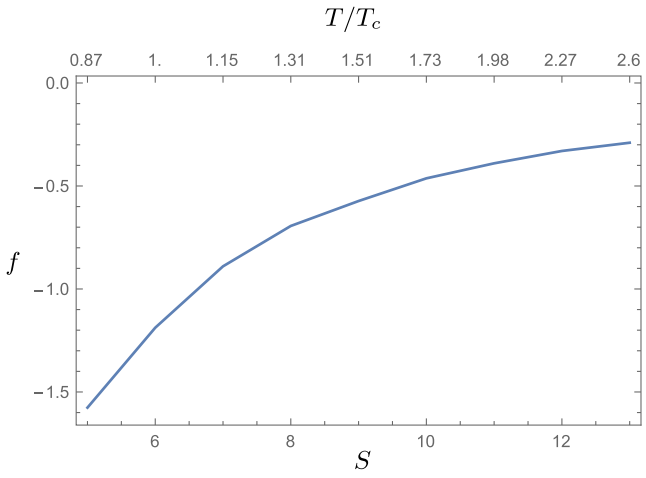

FIG. 9 (color online). Self-consistent value of the Free energy density f as a function of action S (lower scale) which is related to T/T_c (upper scale).

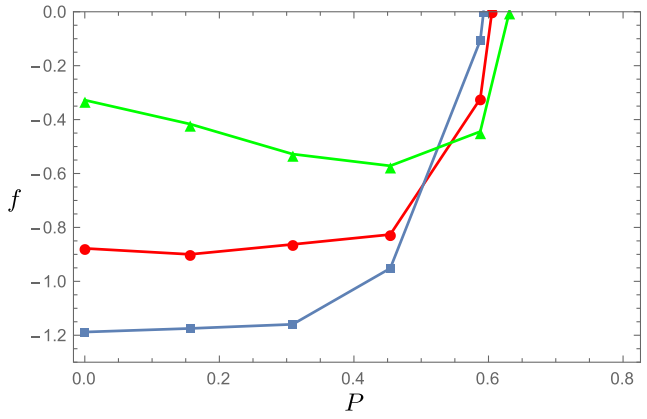

FIG. 10 (color online). (Not-self-consistent in holonomy ν) free energy density f, here shown as a function of the value of the holonomy (in form of the Polyakov loop P) at $S = 6, 7, 9$. The lower the action the lower the minimum of the free energy.

We start this work with an idealized classical solution minimizing classical Yang-Mills action, the BPS soliton, with zero holonomy potential. Quantum fluctuations in one-loop order generate the GPY potential. Furthermore, our ensemble of many dyons also contribute, resulting in a potential displaying confinement. The calculated Debye mass is of the right magnitude.

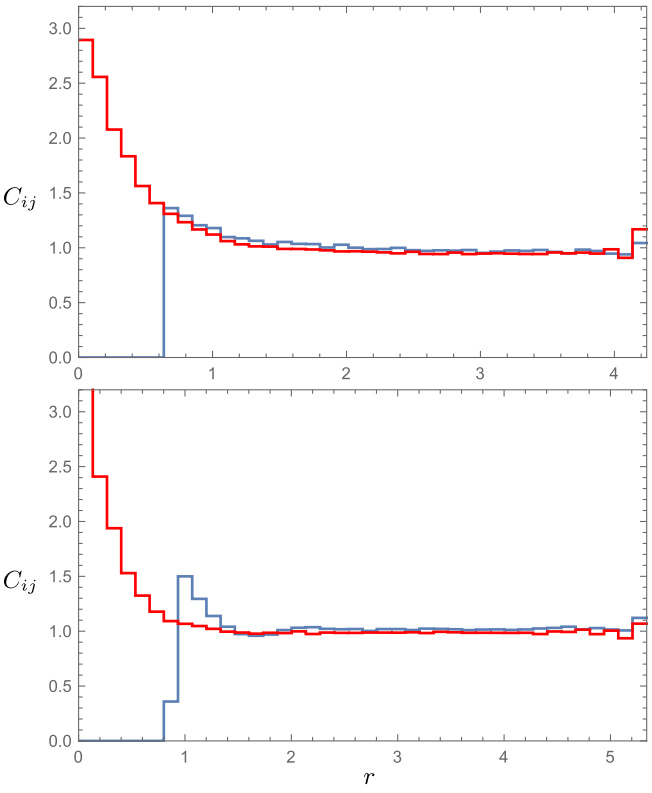

FIG. 11 (color online). Correlation function C_{ij} for MM and ML for $S = 6$ (upper) and $S = 9$ (lower). In the MM case the correlation function vanishes at small distances due to the core.

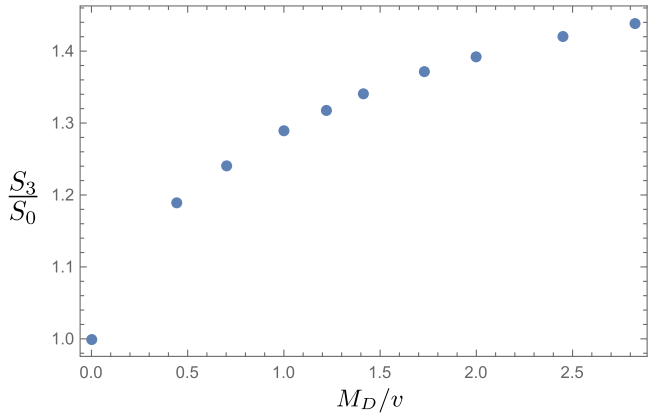

FIG. 12 (color online). Action S_3 of a single dyon as a function of Debye mass over holonomy M_D/v in the potential described by Eq. (26) normalized by the action S_0 for $M_D = 0$.

One may now wonder how the presence of the holonomy potential affects the dyon solution itself. Let us add a (simplified) potential

$$V_{M_D} = \frac{M_D^2}{2}(v - Tr(\tau_3 U_4))^2 \tag{26}$$

and look for the action minimum. For technical reasons, instead of solving nonlinear differential equations, we minimized the action using the gradient flow for a single dyon on the lattice. The resulting action as a function of the Debye mass is shown in Fig. 12 and the shape of the solutions in Fig. 13. One can see, that the role of a nonzero Debye mass is to suppress the tails of the fields. This, in turn, somewhat increases the action.

To illustrate the effect of the increased dyon action on the ensemble, consider an example. For the confined holonomy $\nu = 0.5$ at T_c with $M_D = 2.2$ we get an action of 35 per dyon, compared to 28 for $M_D = 0$. As a result the free density of dyons becomes 1.7 times smaller.

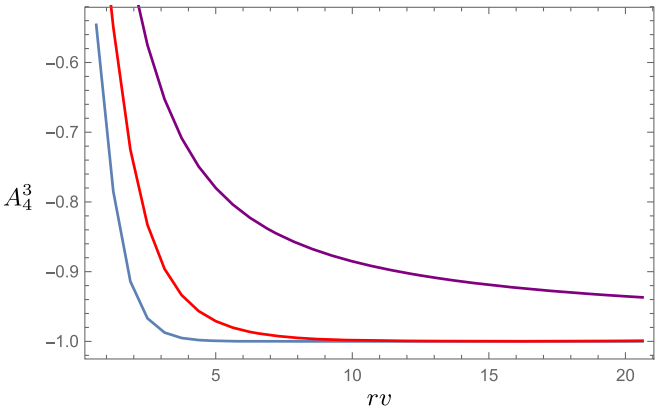

FIG. 13 (color online). Higgs field A_4^3 of a single dyon, along the z-axis, through the center of the dyon for different Debye masses. From top to bottom: $M_D/v = 0$, $M_D/v = 0.45$ and $M_D/v = 1.41$.

Further improvements may be done including higher order quantum corrections. We have just demonstrated that the action and size of a dyon are modified by the holonomy potential. Obviously, other ingredients, such as the zero mode metric and the nonzero mode determinant, are modified as well. In principle, it is known how to approach this problem: since our configurations are already defined on the lattice, one can switch in quantum fluctuations, following standard lattice definition. A variant of the lambda-trick can produce the value of quantum corrections to the deformed non-BPS dyons as well. At this point this calculation is not yet done.

The reason we mention it here is related with the following comment. For the pure holonomy field, $A_4 \neq 0$, in the bulk, the field strengths and thus classical action are zero. The GPY potential is nonzero as a result of a one loop calculation [2]. Two-loop correction has been calculated recently [22] and the result is proportional to the first order result, with the factor $1 - 5/S + \cdots$, where $S = 8\pi^2/g^2$. One finds therefore that for the values of the parameter $S \sim 6$–10 we work with, this two-loop correction is not small: so the holonomy itself is *not* classical, it is subject to strong quantum fluctuations.

Two-loop and three-loop corrections to instantons are only calculated so far in quantum mechanical models, and similar calculations for gauge theory instants and dyons are of interest. We do not expect those to be as large as for the holonomy potential: in quantum mechanics it is of the type $1 - 1/S$ instead.

IX. SUMMARY AND DISCUSSION

As emphasized in the Introduction, an idea that it should be possible to understand confinement (as well as chiral symmetry breaking) via statistical mechanics in terms of collective coordinates of certain topological solitons goes back to the 1970s. Four decades later we now are able to calculate the contribution of the topology to the holonomy potential and explain why its minimum shifts to the confining value at $T < T_c$.

In particular, by identifying classical interaction between instanton-dyons [15] and including them in direct Monte-Carlo simulation of the ensemble, together with one-loop effects in the measure, we calculated the free energy as a function of all parameters of the model, such as the value of the holonomy, dyon densities, and the Debye mass. We then proceed to one-parameter set of its minimum, corresponding to dependence on the only left variable, the temperature. The results display the deconfinement transition at a certain density of the dyons. The key to this is the volumes of the dyon repulsive cores, which scale as an inverse cube of the holonomy.

One of the key questions is whether the objects we study are sufficiently semiclassical. The action per M dyon, $S\nu$, varies in the region studied in this work in the range from 2.5 to 3.3. Its exponent $\exp(-S\nu)$ varies between 0.082 and 0.037. The input formula we use include classical and one-loop effects. By selecting specially tuned Λ parameter, one basically includes the two-loop effects as well. So, we think that the accuracy of these expressions $O(1/S)$ is sufficient for our purposes.

Direct simulations of the ensemble have no general approximations, and the accuracy of the results is limited by size of the system and the statistical errors of the Monte Carlo sampling. We demonstrated in this work that the ensemble of instanton-dyons, coupled to holonomy, does undergo a deconfinement phase transition at a certain value of their density. It is physically driven by repulsive interactions, which enforce "equality" between M and L dyons, broken in the dilute regime by their different actions. We see how it happens in detail: first by performing multiple simulations as a function of all parameters of the model—dyon densities, holonomy, the value of the Debye mass—and then identifying a codimension 1 set of the free energy minima, corresponding to physical dyon ensemble as a function of the temperature T. All these results—the holonomy potential and the mean Polyakov line $\langle P(T)\rangle$, the dyon densities $n_M(T)$, $n_L(T)$ can and should be compared to the lattice data.

This approach can straightforwardly be generalized to the QCD-like theories with an arbitrary number of colors and quark flavors. We plan to do larger scale simulations of those in subsequent publications.

Finally, let us address a very general question often asked: why should one study statistical mechanics of some solitons, rather than directly simulate gauge fields on the lattice, from the first principles?

Quantum field theories have infinitely many degrees of freedom, and an understanding of which ones are responsible for a particular phenomenon is very important. Using an analogy to condense matter physics: One can in principle do direct simulations of all electrons in a piece of metal. And yet, understanding the zone structure, location and shape of the Fermi surfaces offers much simpler and more intuitive approaches to metal thermodynamics and kinetics. To a large extent, the same is true for quarks in the "zero mode zone" of the topological solitons. Now we see that instanton-dyons generate confinement as well as chiral symmetry breaking. The model we use has only few variables per fm^3 volume, 5–6 orders of magnitude less than current lattice simulations.

ACKNOWLEDGMENTS

This work was supported in part by the U.S. Department of Energy, Office of Science under Contract No. DE-FG-88ER40388.

APPENDIX A: UNITS AND HOLONOMY

The main physical quantity of the problem is the temperature T: it defines the magnitude of the

$A_4^3 = 2\pi\nu T$ (holonomy), the physical size of the dyons and every other dimensional parameter of the problem. Yet, precisely because of its omnipresence in the theory at its classical level, dealing only with the dimensionless quantities—e.g. the dyon density normalized as n/T^3—one can in *zeroth* approximation cancel all powers of T. At this level, our theory has only dimensionless input parameters. Most of them—the dimensionless *dyon densities*, *holonomy* and the *Debye screening mass*—will be defined self-consistently, from the minimum of the free energy. The remaining input will be the *instanton action parameter* S, used in many plots in the text.

Standard Euclidean formulation of the gauge theory at finite temperature T introduces periodic (Matsubara) time τ defined on a circle with a period equal to the inverse temperature $1/T$. The exponential of the gauge invariant integral over this circle, known as the Polyakov line

$$P = \frac{1}{N_c} TrP \exp\left[i \oint A_4^3 (\sigma^3/2) d\tau \right], \tag{A1}$$

which is gauge invariant due to periodicity. Here σ^3 is the 3rd Pauli matrix.

As a function of temperature its expectation value $\langle P \rangle$ changes from 1 at high T to (near) zero at the deconfinement temperature T_c. In the simplest SU(2) gauge theory we will discuss in this work $\langle P \rangle = \cos(\nu\pi)$, and the holonomy parameter (or just holonomy, for short) ν changes from 0 to $1/2$. What remains unknown is the physical origin of this potential.

Perturbatively, the effect of the holonomy is the appearance of nonzero masses of quarks and (nondiagonal) gluons, and the corresponding Gross-Pisarski-Yaffe holonomy potential [2]

$$\frac{V_{\rm GPY}(\nu)}{T^4 V_3} = \frac{(2\pi)^2 \nu^2 \bar{\nu}^2}{3}, \tag{A2}$$

where V_3 is the 3-volume of the box and

$$\bar{\nu} = 1 - \nu \tag{A3}$$

is "dual holonomy." We proceed in the text to use dimensionless units for volume $\tilde{V}_3 = T^3 V_3$, densities $n_M = \frac{N_M}{\tilde{V}_3}$, $n_L = \frac{N_L}{\tilde{V}_3}$, distances $rT = x$ and free energy density $\frac{F}{T\tilde{V}_3} = f$. Potential $V_{\rm GPY}$ has a minimum at trivial holonomy $\nu = 0$ and a maximum at confining holonomy $\nu = 1/2$, thus disfavoring confinement.

In the *next* approximation the so-called quantum loop effects are incorporated. As is well known, they lead to a running coupling constant. Thus the action parameter (and all others, of course) become a function of the basic physical scale given by the temperature T. For example, recalling classical instanton action and the asymptotic freedom formula

$$S(T) = \frac{8\pi^2}{g^2(T)} = b \cdot \ln\left(\frac{T}{\Lambda}\right), \qquad b = \frac{11}{3} N_c, \tag{A4}$$

with the power given by the one-loop beta function. If so, the semiclassical factors defining the caloron density now depend on T, basically as a power

$$\frac{n_{\rm calorons}(T)}{T^4} \sim e^{-S} \sim \left(\frac{\Lambda}{T}\right)^b. \tag{A5}$$

Since the caloron density has been measured on the lattice at different T, one can test this expression against the lattice data. In fact it does work, see Fig. 1 of Ref. [14], which confirms that the topological solitons remain semiclassical at the temperatures we discuss.

The next question is the value of the parameter Λ in the expression for S above. Note, that our parameter Λ is proportional to that in multiple other definitions, such as $\Lambda_{\rm lattice}$ or $\Lambda_{\bar{M}S}$, but is not equal to them. In principle, the relation between them is known, and the reader may thus ask why we do not use such relations, obtained from the first principles. The answer is pragmatic: we believe that the current accuracy of them raised in high power, e.g. $\Lambda^b_{\bar{M}S}$, is still lower than what was found from the fit to the caloron data just mentioned. In other words, the measurements of the caloron density is basically the measurements of the high power of Λ, and they thus provide more accurate values than what can possibly be done by (much more accurate) measurements but of quantities depending on this parameter logarithmically.

Not surprisingly, in practice the meaning (and the value) of Λ depends on the context in which it is used. The fit shown in Fig. 1 of Ref. [14] corresponds to noninteracting gas of calorons, and it gives

$$\Lambda_{\rm calorons} = 0.36 T_c, \tag{A6}$$

where T_c is the deconfinement transition temperature, defined in the same lattice work. If so, the (instanton action) parameter is $S \approx 7.5$ at T_c.

In our work we worked out a much more sophisticated model of the interacting dyon plasma. In this model the deconfinement transition happens at a somewhat different value of the (instanton action) parameter $S \approx 6$. In other words,

$$\Lambda_{\rm dyonic\ plasma} = 0.44 T_c. \tag{A7}$$

This value is assumed in all plots in Sec. VII in which our input parameter S is mapped to the temperature T.

The reader should however keep in mind, that this mapping between the input parameter of the model S

and physical T is provisional, it depends on the model itself. No doubt it should be subject to future improvements, both in the lattice data quality used for such fits, or the fit itself. In particular, one should include measurements of the instanton-dyons, including the effects of their interaction as discussed in the bulk of our paper.

APPENDIX B: INSTANTON-DYONS

We do not present here extensive introduction on the configurations and their history, which can be found in literature such as [12].

"Higgsing" the SU(2) gauge theory by nonzero VEV of A_4 called v leads to two massive and one massless gluons. The simplest gauge is the so called regular (hedgehog) gauge, in which the color direction of the "Higgs" field is at large r along the unit radial vector $A_4^m \to v\hat{r}^m$. The solutions are

$$A_4^a = \pm\hat{r}_a\left(\frac{1}{r} - v\coth(vr)\right)$$
$$A_i^a = \epsilon_{aij}\hat{r}_j\left(\frac{1}{r} - \frac{v}{\sinh(vr)}\right). \tag{B1}$$

$+$ corresponds to the M dyon and $-$ corresponds to the $\bar{M}$ dyon. r is the length in position space. The L and $\bar{L}$ dyon are obtained by a replacement $v \to 2\pi T - v$. To study the classical interaction of the dyons, a gauge transformation is done to make A_4 field point in a specific direction (normally this is chosen to be A_4^3), which introduced a time dependence in the L dyons in order to compensate for the extra $2\pi T$. The classical interaction between the dyons can at long range be described by the same formula for all

$$V(r) = \frac{8\pi^2\nu}{g^2}\left((e_1e_2 - 2h_1h_2)\frac{1}{x} + m_1m_2\frac{1}{x}\right)$$
$$x = 2\pi\nu r. \tag{B2}$$

e, m, h are listed in the Table I.

As a result sectors that are completely self-dual or anti-self-dual have no interaction, while dyons and antidyons of same type attract and dyons and antidyons of different type repel.

TABLE I. Quantum numbers of the four different kinds of the instanton-dyons of the SU(2) gauge theory. The first two rows are electric and magnetic charges, while by h we mean the contribution from nonlinear terms including the holonomy field.

	M	$\bar{M}$	L	$\bar{L}$
e	1	1	-1	-1
m	1	-1	-1	1
h	1	1	-1	-1

APPENDIX C: THE DYON WEIGHTS IN THE PARTITION FUNCTION

The KvBLL caloron partition function [20] has the form

$$Z_{\mathrm{KvBLL}} = \int d^3z_1 d^3z_2 T^6 C\left(\frac{8\pi^2}{g^2}\right)(e^{-\frac{8\pi^2}{g^2}})\left(\frac{1}{Tr_{12}}\right)^{\frac{5}{3}} \times (2\pi + 4\pi^2\nu\bar{\nu}Tr_{12})(2\pi\nu Tr_{12} + 1)^{\frac{8\nu}{3}-1} \times (2\pi\bar{\nu}Tr_{12} + 1)^{\frac{8\bar{\nu}}{3}-1}\exp\left(-V_3T^3\frac{4\pi^2}{3}\nu^2\bar{\nu}^2\right). \tag{C1}$$

Taking the limit to a very dilute situation we find that all powers of Tr_{12} not in the exponential cancel, and we end with

$$Z_{\mathrm{KvBLL}} = \int d^3z_1 d^3z_2 T^6 C\left(\frac{8\pi^2}{g^2}\right)(e^{-\frac{8\pi^2}{g^2}}) \times (2\pi\nu)^{\frac{8\nu}{3}}(2\pi\bar{\nu})^{\frac{8\bar{\nu}}{3}} \times \exp\left(-V_3T^3\frac{4\pi^2}{3}\nu^2\bar{\nu}^2\right). \tag{C2}$$

The term in the exponential corresponds to the GPY holonomy potential in Eq. (A2). The Diakonov determinant, which we have included, is seen to return to a product of the holonomies in the dilute limit

$$\lim_{Tr_{12}\to\infty}\det G = \prod_i 4\pi\nu_i. \tag{C3}$$

By comparison we see that we have to take Eq. (C2) and divide by Eq. (C3) in order to get the correct weight for our partition function. We thus end up with the partition function for a M and L dyon given by

$$Z_{\mathrm{KvBLL}} = \int d^3z_1 d^3z_2 T^6 C\left(\frac{8\pi^2}{g^2}\right)(e^{-\frac{8\pi^2}{g^2}}) \times \frac{(2\pi)^{8/3}}{(4\pi)^2}\nu^{\frac{8\nu}{3}-1}\bar{\nu}^{\frac{8\bar{\nu}}{3}-1} \times \exp\left(-V_3T^3\frac{4\pi^2}{3}\nu^2\bar{\nu}^2\right). \tag{C4}$$

We redefine the constant Λ so the equation is easier to work with

$$Z_{\mathrm{KvBLL}} = \int d^3z_1 d^3z_2 T^6\frac{\Lambda^2}{(4\pi)^2}\left(\frac{8\pi^2}{g^2}\right)^4 e^{-\frac{8\pi^2}{g^2}} \times \nu^{\frac{8\nu}{3}-1}\bar{\nu}^{\frac{8\bar{\nu}}{3}-1}\exp\left(-V_3T^3\frac{4\pi^2}{3}\nu^2\bar{\nu}^2\right). \tag{C5}$$

[1] E. V. Shuryak, Quantum chromodynamics and the theory of superdense matter, Phys. Rep. **61**, 71 (1980).
[2] D. J. Gross, R. D. Pisarski, and L. G. Yaffe, QCD and instantons at finite temperature, Rev. Mod. Phys. **53**, 43 (1981).
[3] A. A. Belavin, A. M. Polyakov, A. S. Schwartz, and Yu. S. Tyupkin, Pseudoparticle solutions of the Yang-Mills equations, Phys. Lett. B **59**, 85 (1975).
[4] T. Schafer and E. V. Shuryak, Instantons in QCD, Rev. Mod. Phys. **70**, 323 (1998).
[5] M. Wagner, Classes of confining gauge field configurations, Phys. Rev. D **75**, 016004 (2007).
[6] F. Lenz, J. W. Negele, and M. Thies, Confining effective theories based on instantons and merons, Ann. Phys. (Amsterdam) **323**, 1536 (2008).
[7] D. Chen, R. C. Brower, J. W. Negele, and E. V. Shuryak, Heavy quark potential in the instanton liquid model, Nucl. Phys. B, Proc. Suppl. **73**, 512 (1999).
[8] P. Gerhold, E.-M. Ilgenfritz, and M. Muller-Preussker, An SU(2) KvBLL caloron gas model and confinement, Nucl. Phys. **B760**, 1 (2007).
[9] J. Greensite, The confinement problem in lattice gauge theory, Prog. Part. Nucl. Phys. **51**, 1 (2003).
[10] T. C. Kraan and P. van Baal, Monopole constituents inside SU(n) calorons, Phys. Lett. B **435**, 389 (1998).
[11] K.-M. Lee and C.-h. Lu, SU(2) calorons and magnetic monopoles, Phys. Rev. D **58**, 025011 (1998).
[12] D. Diakonov, Topology and confinement, Nucl. Phys. B, Proc. Suppl. **195**, 5 (2009).
[13] E. Poppitz, T. Schafer, and M. Unsal, Universal mechanism of (semi-classical) deconfinement and theta-dependence for all simple groups, J. High Energy Phys. 03 (2013) 087.
[14] E. Shuryak and T. Sulejmanpasic, Holonomy potential and confinement from a simple model of the gauge topology, Phys. Lett. B **726**, 257 (2013).
[15] R. Larsen and E. Shuryak, Classical interactions of the instanton-dyons with antidyons, arXiv:1408.6563.
[16] Y. Liu, E. Shuryak, and I. Zahed, Confining dyon-anti-dyon Coulomb liquid model I, Phys. Rev. D **92**, 085006 (2015).
[17] P. Faccioli and E. Shuryak, QCD topology at finite temperature: Statistical mechanics of self-dual dyons, Phys. Rev. D **87**, 074009 (2013).
[18] F. Bruckmann, S. Dinter, E. M. Ilgenfritz, M. Muller-Preussker, and M. Wagner, Cautionary remarks on the moduli space metric for multi-dyon simulations, Phys. Rev. D **79**, 116007 (2009).
[19] A. Cosnuau, Computation on GPU of eigenvalues and eigenvectors of a large number of small Hermitian matrices, Procedia Comput. Sci. **29**, 800 (2014).
[20] D. Diakonov, N. Gromov, V. Petrov, and S. Slizovskiy, Quantum weights of dyons and of instantons with nontrivial holonomy, Phys. Rev. D **70**, 036003 (2004).
[21] V. G. Bornyakov and V. K. Mitrjushkin, SU(2) lattice gluon propagators at finite temperatures in the deep infrared region and Gribov copy effects, Phys. Rev. D **84**, 094503 (2011).
[22] A. Dumitru, Y. Guo, and C. P. K. Altes, Two-loop perturbative corrections to the thermal effective potential in gluodynamics, Phys. Rev. D **89**, 016009 (2014).